Breast Cancer (2018) 25:233–242
https://doi.org/10.1007/s12282-017-0821-9

ORIGINAL ARTICLE

Schisandrin A reverses doxorubicin-resistant human breast cancer cell line by the inhibition of P65 and Stat3 phosphorylation

Zong-Lin Zhang[1] · Qing-Cheng Jiang[2] · Su-Rong Wang[3]

Received: 3 July 2017 / Accepted: 15 November 2017 / Published online: 27 November 2017

Abstract

Background Multidrug resistance (MDR) in breast cancer therapy occurs frequently. Thus, anti-MDR agents from natural products or synthetic compounds were tested extensively. We have also explored the reverse effect and mechanism of Schisandrin A (Sch A), a natural product, on MCF-7 breast cancer doxorubicin (DOX)-resistant subline MCF-7/DOX.

Methods MTT assay was performed to measure the viability of MCF-7 cells to assess the reverse effect of Sch A. Western blot analysis was used to study the protein levels. Laser scanning confocal microscopy was performed to detect the intercellular DOX and Rhodamine 123 accumulation. The qRT-PCR was used to analysis the target gene expression. Dual-luciferase reporter assay was performed to test the transcriptional activity of P-glycoprotein (P-gp).

Results Sch A, at the concentration of 20 μM, showed selective reverse effect (better than the positive control, verapamil at 5 μM) on MCF-7/DOX cell line but not on BEL-7402/DOX, Hep G2/DOX, and K-562/DOX cells. In addition, Sch A enhanced DOX-induced cleavage of Caspase-9 and PARP levels by increasing intracellular DOX accumulation and inhibiting P-gp function. Furthermore, Sch A selectively suppressed P-gp at gene and protein levels in MCF-7/DOX cells which express high level of *MDR1* but not *MRP1*, *MRP3,* or *BCRP*. Besides, Sch A showed inhibitory effect on P-gp transcriptional activity. Sch A significantly reduced p-IκB-α (Ser32) and p-Stat3 (Tyr705) levels which mediate P-gp expression. In addition, Stat3 knockdown enhanced the reverse effect of siP65. The combined effect of siStat3 and siP65 was better than Sch A single treatment in MCF-7/DOX cells.

Conclusion Sch A specifically reverses P-gp-mediated DOX resistance in MCF-7/DOX cells by blocking P-gp, NF-κB, and Stat3 signaling. Inhibition of P65 and Stat3 shows potent anti-MDR effect on MCF-7/DOX cells.

Keywords Multidrug resistance · Doxorubicin · Schisandrin A · NF-κB · Stat3

Introduction

Chemotherapy for breast cancer is often hampered by the rapid emergence of drug resistance, which exists for both conventional chemotherapies and new drugs targeted to mutated or deregulated tumor cells [1, 2]. Diverse mechanisms are associated with the development of multidrug resistance (MDR). The major cause of MDR is attributed to efflux pumps that reduce intracellular drug concentration. The efflux pumps are identified as ATF-binding cassette (ABC) transporters characterized with their homologous ATP-binding domains. P-glycoprotein (P-gp also known as MDR1 or ABCB1) is the most important ABC transporter. Numerous drugs in chemotherapy for breast cancer are the substrates of P-gp, including doxorubicin (DOX), daunorubicin, paclitaxel, vinblastine, vincristine, and etoposide [3]. Notably, MDR-associated protein 1 (MRP1), MRP3, and breast cancer resistance protein (BCRP), which are three eminent ABC transporters that modulate anticancer drug uptake and efflux, do not correlate as closely as P-gp with an MDR phenotype [4].

DOX acts through topoisomerase II by stabilizing the intermediary "cleavage DNA" product of topoisomerase II and inhibiting reconnection. When resistance to DOX treatment occurs, breast cancer may become not only resistant

✉ Su-Rong Wang
wangsrpaper@sina.com

[1] Department of Pharmacy, Linyi People's Hospital, Linyi, Shandong, China

[2] Department of Pharmacy, First People's Hospital of Tancheng County, Tancheng, Shandong, China

[3] Department of Gynecology and Obstetrics, Linyi People's Hospital, 27# Jie fang lu dong duan, Linyi, Shandong, China

to the drug originally administered but also to a wide variety of structurally and mechanistically unrelated drugs [5]. Mechanisms involve the MDR development including decreased drug uptake and increased drug efflux by P-gp, activation of DNA repair mechanisms, mutated targets, evasion of drug-induced apoptosis, activation of detoxifying systems, etc. The plant known as *Fructus schisandra* (FS) in the Chinese Pharmacopoeia, and more commonly known as *Schisandra chinensis* or the five-flavor berry, has been applied as a medicinal herb in China for several millennia without reports of side effects, and is indexed as tonic and sedative. Schisandrin A (Sch A) extracted from FS showed the most potent MDR reversal activity in vitro and in vivo [6]. Another recent study reported that Sch A affected the expression of membrane P-gp and inhibited P-gp efflux capability in the DOX-resistant human osteosarcoma MG-63 cell line (MG-63/DOX) [7]. However, the molecular mechanisms of Sch A to reverse MDR are not well understood in breast cancer.

Nuclear factor kappa-B (NF-κB) signaling is thought to be highly related to P-gp expression [8]. NF-κB is a mediator of inducible gene expression in response to inflammatory cytokines, pathogens, and several stress signals, and is known for its crucial roles in the immune system, cell proliferation and transformation, apoptosis, and tumor development. A constitutive NF-κB activity has been observed in several MDR malignancies. Phosphorylation of inhibitor κB-α (IκB-α) is required for NF-κB activation [9]. A significant increase of p-IκB-α leads to the activation of NF-κB. The previous studies demonstrated that the activation of NF-κB leads to P-gp up-regulation [10]. Thus, inhibition of NF-κB signaling gives rise to down-regulation of P-gp and recovers the sensitivity of MDR carcinomas to chemotherapeutic agents. Constitutive activation of signal transducers and activators of transcription 3 (Stat3) play a critical role in the tumorigenesis and progression of various human malignances [11, 12]. Stat3 activation is highly regulated by intracellular kinases, such as Janus kinases (JAKs) and Src, which are hyperactivated in a wide range of human cancers, including breast cancer [13]. Therefore, inhibition of Stat3 signaling has been suggested to be a promising therapeutic strategy for the treatment of this malignancy.

In this study, we investigated the reversal effect of Sch A on several DOX-resistant carcinomas. Furthermore, MCF-7/DOX cells were used to evaluate the ability of Sch A to increase intracellular DOX and rhodamine 123 (Rh123), and DOX-induced apoptosis. In addition, we measured the effects of Sch A on P-gp levels and investigated the involvement of NF-κB and Stat3 in P-gp regulation.

Materials and methods

Chemicals and reagents

DOX, Sch A, verapamil (VRP), rhodamine 123 (Rh123), 3-(4,5-dimethylthiazol-2-yl)-2,5-diphenyltetrazolium bromide (MTT), and dimethylsulfoxide (DMSO) were purchased from Sigma–Aldrich (St. Louis, MO). NSC 74,859 and ammonium pyrrolidinedithiocarbamate (PDTC) were purchased from ApexBio (Houston, USA). The human MDR1 Luciferase reporter plasmid (hMDR1-Luc) was purchased from Takara (Dalian, China). The PRL-SV40 plasmid was purchased from Promega (Madison, WI). The pNF-κB-luc reporter plasmid and pStat3-TA-luc reporter plasmid were bought from Beyotime (Haimen, China). The proteasome inhibitor MG-132 and the primary antibodies for P-gp, p-P65, p-IκB-α (Ser32), p-Stat3 (Tyr705), cleaved Caspase-9, Caspase-9, cleaved-poly(ADP-ribose) polymerase (PARP), and GAPDH were purchased from Cell Signaling Technology (Danvers, MA). Other reagents and chemicals were of analytical grade purity.

Cell lines, cell culture, and treatments

BEL-7402, K-562 and MCF-7, and their DOX-resistant sublines BEL-7402/DOX, K-562/DOX, and MCF-7/DOX were obtained from KeyGEN (Nanjing, China), and maintained in RPMI-1640 supplemented with 10% fetal bovine serum (FBS). Hep G2 and its DOX-resistant subline Hep G2/DOX were purchased from BeNa Culture Collection (Beijing, China), and cultured in RPMI-1640 supplemented with 10% FBS. All DOX-resistant sublines were maintained in culture medium containing 1000 ng/mL DOX and incubated in drug-free medium for at least 1 week before use.

Cell viability assay

Cell viability assay was performed as described previously [14].

Cytotoxicity assay

Chemosensitivity to DOX was determined using MTT colorimetric assay as described previously [7]. Cells were treated with a full range of concentrations of DOX with or without 20 or 50 μM Sch A or 5 μM VRP for 48 h. The absorbance in each well was read at 570 nm with background subtraction at 630 nm using a microplate reader

(molecular devices). IC_{50} values were calculated from survival curves using the Bliss method [15].

Intracellular DOX fluorescence assay

Intracellular DOX accumulation was measured by laser scanning confocal microscopy (LSCM), as previously described [7]. MCF-7 and MCF-7/DOX cells were treated with 5 μM DOX for 12 h in the absence or presence of 20 μM Sch A or 5 μM VRP (positive control). Then, cells were washed twice with PBS and fixed in 4% paraformaldehyde for 10 min, and washed three times with PBS, and the fluorescence intensity of intracellular DOX was measured. Intracellular DOX was quantified using Image Pro Plus 6.0 (Media Cybernetics, Inc., Rockville, MD, USA).

Intracellular Rh123 fluorescence assay

MCF-7 and MCF-7/DOX cells were pretreated with or without 20 μM Sch A or 5 μM VRP (positive control) for 1 h and then incubated with 5 μM Rh123 in the dark for 12 h. Then, cells were washed twice with PBS and fixed in 4% paraformaldehyde for 10 min, and washed three times with PBS, and the fluorescence intensity of intracellular Rh123 was measured. Intracellular Rh123 was quantified using Image Pro Plus 6.0 (Media Cybernetics, Inc., Rockville, MD, USA).

Quantitative real-time RT-PCR

The quantitative real-time polymerase chain reaction (qRT-PCR) was performed as previously described [16]. The Δ cycle threshold method was used for the calculation of relative differences in mRNA abundance with a LightCycler 480 (Roche Molecular Biochemicals, Mannheim, Germany). Data were normalized to the expression of *GAPDH*. The results of real-time RT-PCR were expressed as fold-changes. The normalized value of the target mRNA of the control group is arbitrarily presented as 1. The sequences of primers used were as follows: *MDR1*, 5′-AGAGTCAAGGAG CATGGCAC-3′ (sense) and 5′-ACAGTCAGAGTTCAC TGGCG-3′ (antisense); *MRP1*, 5′- TAATCCCTGCCC AGAGTCCA-3′ (sense) and 5′- ACTTGTTCCGACGTG TCCTC-3′ (antisense); *MRP3*, 5′-TTCTACGGGATGGCC AGAGA-3′ (sense) and 5′-CGGAATCCGGCAAGTCCA TT-3′ (antisense); *BCRP*, 5′- AGATTGAGAGACGCGGCA AG-3′ (sense) and 5′- CACCCGGACCTTCCAAACAA-3′ (antisense); and *GAPDH*, 5′-GAAAGCCTGCCGGTGACT AA-3′ (sense) and 5′-AGGAAAAGCATCACCCGGAG-3′ (antisense).

Western blot analysis

Protein of 20 or 38 μg was used for SDS polyacrylamide gel electrophoresis. After transfer to PVDF membrane, the proteins were reacted with antibodies (Cell Signaling Technology, Danvers, MA) indicated in the figures followed by anti-rabbit IgG conjugated to horseradish peroxidase (Jackson Laboratories, West Grove, PA). EasySee Western Blot Kit (TransGen Biotech, Beijing, China) was used to determine the levels of protein expression. Immunoreactive protein bands were detected with a ChemiDOC XRS+ (Bio-Rad Inc., Hercules, CA). Image Lab 4.0 (Bio-Rad, Inc., Hercules, CA) was used to quantify protein expression based on band intensity.

Dual-luciferase reporter assay

The *MDR1*-promoter reporter plasmid preparation was performed and as previously described [8] with some modifications. MCF-7/DOX cells were transfected using Opti-MEM (Life Technologies, Grand Island, NY) containing 10 μg plasmids and Super Electroporator NEPA21 system (NEPAGENE, Japan). Thirty-six hours after transfection, cells were treated with 0–30 μM Sch A for 12 h to test *MDR1*-promoter activity or 8 h to detect NF-κB or Stat3 activity.

Small interfering RNA

The siRNA sequences used for transient transfections were previously described [17]. P65 siRNA (h) was purchased from Santa Cruz Biotechnology (Dallas, TX, USA); siStat3 is 5′-GGGACCUGGUGUGAAUUAUdTdT-3′ and siNC is 5′-UUCUCCGAACGUGUCACGUdTdT-3′. Transfection was performed using the Super Electroporator NEPA21 system [16]. Briefly, 1×10^6 MCF-7/DOX cells were transfected using Opti-MEM containing 150 pM siRNA oligos. After 48 h later, cells were used for Western blot detection or treated with DOX for 48 h, followed by MTT assay.

Statistical analysis

All quantitative results were reported as mean ± S.D. of the data from at least three experiments performed in a parallel manner. Statistical analysis was performed with the GraphPad Prism 5 software.

Results

Sch A selectively reverses MCF-7/DOX resistance

To determine the anti-proliferative effects of Sch A (Fig. 1a) and VRP, we tested the cell viability of MCF-7 and its

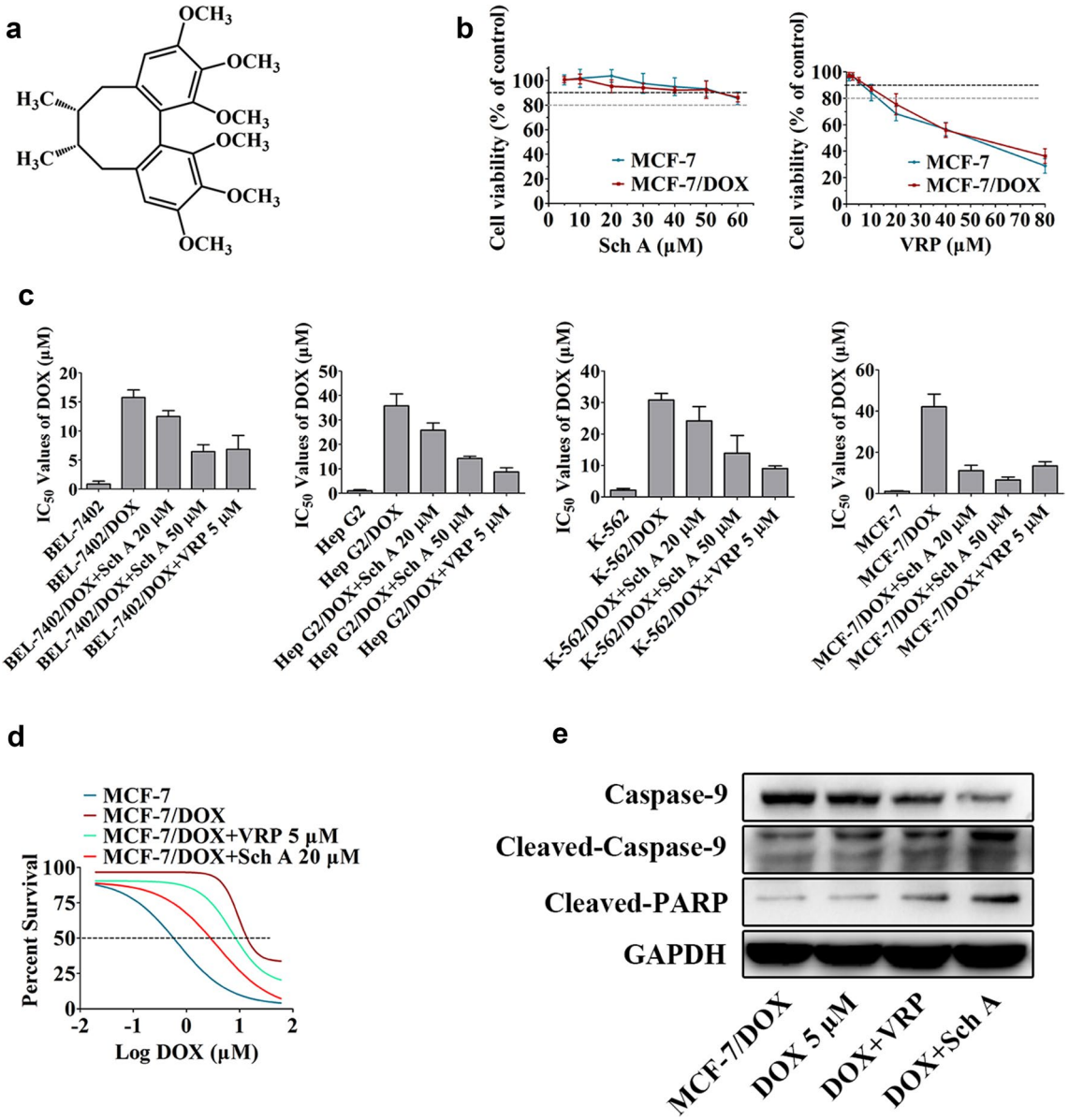

Fig. 1 Sch A selective reverses DOX-resistant MCF-7 cells. **a** Chemical structure of Sch A. **b** MCF-7 or MCF-7/DOX cells were incubated with 0–60 μM Sch A or 0–80 μM VRP for 48 h. The cell viability was measured by the MTT assay. **c** Full range of concentrations of DOX with or without Sch A (20 or 50 μM, 48 h) or VRP (5 μM, 48 h) was added to the four kinds of cancer cell lines or their DOX-resistant sublines. The IC_{50} values of DOX were measured by the MTT assay. **d** To measure the cytotoxicity of DOX in parental and drug-resistant cells, MCF-7 and MCF-7/DOX cells were treated with various concentrations of DOX with or without 5 μM VRP or 20 μM Sch A for MTT assay. **e** Western blot results of the whole-cell lysates. MCF-7/DOX cells treated with or without 5 μM DOX combined with or without 20 μM Sch A or 5 μM VRP for 48 h for the detection of cleaved caspase-9 and cleaved PARP with GAPDH as loading control

DOX-resistant subline MCF-7/DOX in the presence of Sch A or VRP. MTT assay indicates that Sch A at concentrations lower than 50 μM did not significantly inhibit the growth of MCF-7 or MCF-7/DOX cells (cell viability > 90%). However, VRP at 10 μM showed a slight inhibitory effect on MCF-7 parental or resistant subline (cell viability < 90%) (Fig. 1b).

To test the reverse activity of Sch A, four human cancer cell lines (BEL-7402, Hep G2, K-562 and MCF-7) and their DOX-resistant sublines (BEL-7402/DOX, Hep G2/DOX, K-562/DOX, and MCF-7/DOX) were treated with various dosages of DOX in the presence or absence of Sch A at 20 or 50 μM, or VRP 5 μM for 48 h. The IC_{50} values of DOX-resistant sublines for DOX were significantly increase than their parental sensitive cell lines. BEL-7402/DOX and BEL-7402: 15.75 ± 1.29 and 0.85 ± 0.50 μM, Hep G2/DOX and Hep G2: 35.78 ± 4.89 and 0.97 ± 0.44 μM, K-562/DOX and

K-562: 30.77 ± 2.11 and 2.12 ± 0.56 μM, MCF-7/DOX and MCF-7: 42.10 ± 6.20 and 1.05 ± 0.30 μM. Sch A showed remarkably reversal effect on MCF-7/DOX (Sch A 20 μM: 11.13 ± 2.56 μM, Sch A 50 μM: 6.54 ± 1.47 μM and VRP 5 μM: 13.36 ± 2.11 μM) but not on BEL-7402/DOX, Hep G2/DOX and K-562/DOX compared with VRP (Fig. 1c, d).

In addition, cleavage of Caspase-9 and PARP served as indicators of the activation and onset of apoptosis. As shown in Fig. 1e, Sch A increased levels of cleaved Caspase-9 and PARP induced by DOX compared with the other groups. These results indicate that Sch A enhances DOX-induced apoptosis and selectively reverses MCF-7/DOX resistance.

Sch A increases DOX accumulation in MCF-7/DOX

We then investigated the manner in which Sch A enhanced DOX-induced cell death by LSCM. The accumulation of DOX in MCF-7/DOX cells was measured. The results showed that compared with DOX alone or DOX combined with VRP, Sch A significantly increased intracellular DOX accumulation (Fig. 2a). DOX is a substrate of P-gp [16]. We speculated that P-gp may play an important role in

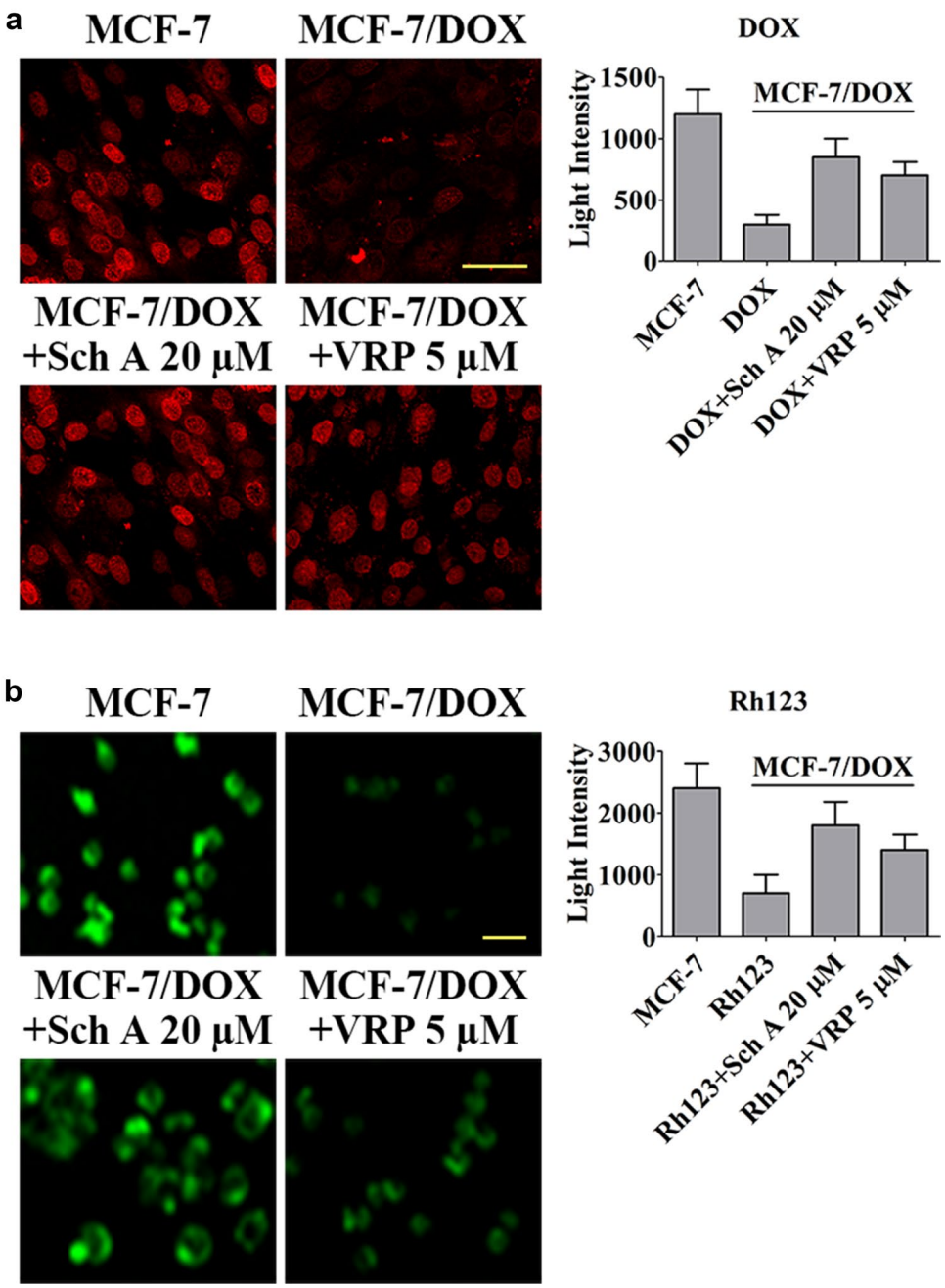

Fig. 2 Sch A increases DOX accumulation by blocking P-gp function in MCF-7/DOX cells. **a** MCF-7 or MCF-7/DOX cells were incubated for 12 h in a medium containing 5 μM DOX with or without 20 μM Sch A or 5 μM VRP, washed three times with PBS and fixed in 4% paraformaldehyde for 10 min at 25 °C, then washed three times with PBS and examined for the fluorescence of intracellular DOX. **b** MCF-7 or MCF-7/DOX cells were pretreated with or without 20 μM Sch A or 5 μM VRP (positive control) for 1 h and then incubated with 5 μM Rh123 in the dark for 12 h. Then cells were washed twice with PBS and fixed in 4% paraformaldehyde for 10 min, and washed three times with PBS, and the fluorescence intensity of intracellular Rh123 was measured. Scale bar 30 μM (**a**) and Scale bar 20 μM (**b**)

DOX efflux. Therefore, we investigated the effect of Sch A on P-gp function by detecting the accumulation of P-gp-specific substrate Rh123. Rh123 uptake occurs via passive inward diffusion, while its efflux is P-gp dependent. As a result, Rh123 has been used extensively as an indicator of P-gp activity [7]. LSCM analysis indicated that MCF-7/DOX cells contained much less Rh123 than did MCF-7 cells. The accumulation of Rh123 in MCF-7/DOX cells treated with Sch A was higher than that in positive control (VRP) cells (Fig. 2b). Not surprisingly, the light intensity of DOX or Rh123 showed notably decrease in MCF-7/DOX compared with MCF-7 cells (Fig. 2). These data suggest that Sch A enhanced the cytotoxicity of DOX by increasing intracellular concentrations of DOX and reduced the efflux of DOX by inhibiting P-gp function in MCF-7/DOX cells.

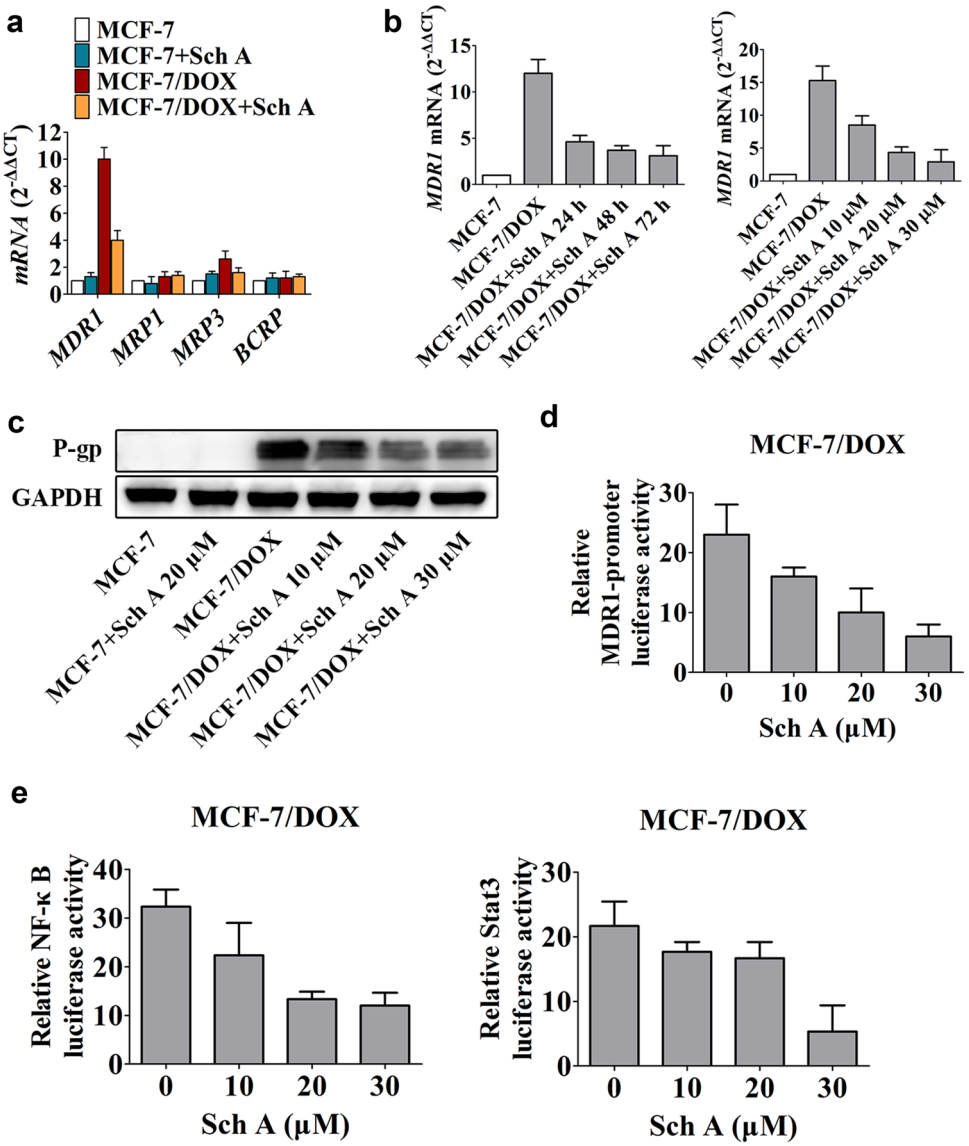

Fig. 3 Sch A suppresses P-gp selectively induced by DOX in MCF-7/DOX cells at gene and protein level. **a** MCF-7 or MCF-7/DOX cells were treated with 20 μM Sch A for 24 h. *MDR1*, *MRP1*, *MRP3,* or *BCRP* mRNA levels were detected by qRT-PCR. **b** MCF-7 or MCF-7/DOX cells were treated with 20 μM Sch A for 0–72 h, or 0–30 μM Sch A for 24 h. *MDR1* mRNA levels were detected by qRT-PCR. The Δ cycle threshold method was used for the calculation of relative differences in mRNA abundance. Data were normalized to the expression of *GAPDH*. The results of real-time RT-PCR were expressed as fold-changes. The normalized value of the target mRNA of the control group is arbitrarily presented as 1. **c** Western blot results of the membrane lysates from the MCF-7 or MCF-7/DOX cells treated with 0–30 μM Sch A for 48 h. **d** MCF-7/DOX cells were co-transfected transiently with the human MDR1 luciferase reporter plasmid and the pRL-SV40 plasmid and 36 h later were treated with 0–30 μM Sch A for 12 h prior to harvesting. **e** MCF-7/DOX cells were co-transfected transiently with the human pNF-κB-luc reporter plasmid or pStat3-TA-luc reporter plasmid and the pRL-SV40 plasmid and 36 h later were treated with 0–30 μM Sch A for 8 h prior to harvesting

Sch A inhibits P-gp which is mainly overexpressed in MCF-7/DOX at gene and protein level

We found that P-gp gene and protein levels in MCF-7/DOX cells were significantly higher than that in its parental sensitive cell line (Fig. 3a, group 1 and 3, 3b, columns 1 and 2, and 3c, lanes 1 and 3). We are interested in the expression of other multidrug-resistant proteins in MCF-7/DOX cells. The results detected by qRT-PCR indicated that P-gp mRNA (*MDR1*) levels, but not *MRP1* [18], *MRP3* [19], or *BCRP* [20], is dramatically up-regulation in MCF-7 DOX-resistant subline (MCF-7/DOX). Sch A showed little effect on MCF-7 cells, but significantly decreased the *MDR1* levels in MCF-7/DOX cells (Fig. 3a). Furthermore, *MRP3* expression showed a slight increase in MCF-7/DOX cells. In addition, Sch A showed negative effect on *MRP1*, *MRP3,* and *BCRP* levels (Fig. 3a). We then investigated the regulatory effect of Sch A on P-gp levels. We found that Sch A at 20 μM inhibited *MDR1* expression in MCF-7/DOX cells in a time-dependent manner (Fig. 3b). In addition, Sch A showed inhibitory effect on P-gp gene and protein expression at 24 and 48 h, respectively, in MCF-7/DOX cells in a concentration-dependent manner (Fig. 3b, c), but not in MCF-7 cells (Fig. 3c). The dual-luciferase reporter experiments indicated that Sch A suppressed *MDR1*-promoter activity in a concentration-dependent manner (Fig. 3d). In addition, Sch A showed potent inhibitory effect on NF-κB and Stat3 activity (Fig. 3e). These results demonstrate that DOX-induced MCF-7 resistant cell line mainly overexpresses P-gp but not MRP1, MRP3, or BCRP. Sch A inhibits P-gp expression in a time-dependent and concentration-dependent manner at gene and protein levels. In addition, Sch A suppresses *MDR1* transcription in a concentration-dependent manner in MCF-7/DOX cells.

Stat3 knockdown enhances the reversal effect of siP65 transfection

NF-κB signaling [21] or Stat3 signaling [22] was reported as a regulator in *MDR1* expression. Thus, the effects of Sch A on IκB-α, P65, and Stat3 phosphorylation were determined in MCF-7/DOX cells. Western blot analysis indicated that IκB-α, P65, and Stat3 phosphorylation were significantly higher in MCF-7/DOX cells than that in parental sensitive MCF-7 cells. The phosphorylation of IκB-α, P65, or Stat3 was subsequently decreased following treatment with Sch A at 48 h in MCF-7/DOX cells in a concentration-dependent manner (Fig. 4a). We further investigated the regulatory effect of NF-κB inhibitor PDTC [7] or Stat3 inhibitor NSC 74859 [17] on P-gp levels. Western blot analysis confirmed that PDTC or NSC 74859 prevented P-gp expression, and PDTC showed more potent inhibitory effect on P-gp levels than NSC 74859 (Fig. 4b, lanes 1 and 2). Sch A had the strongest suppression on P-gp expression (Fig. 4b, lane 3). In addition, Sch A showed inhibitory effect on both IκB-α, P65, and Stat3 phosphorylation in MCF-7/DOX cells, and no wonder, PDTC or NSC 74859 potently restrained p-IκB-α, p-P65, or p-Stat3 levels, respectively (Fig. 4b). These results suggest that inhibition of NF-κB signaling or Stat3 signaling reduces P-gp expression. Phospho-IκB-α and phospho-P65 prevention showed more powerful inhibitory effect on P-gp levels than Phospho-Stat3 suppression. However, Sch A restrains p-IκB-α, p-P65, and p-Stat3, and shows the strongest inhibitory effect on P-gp expression.

We speculate that suppression of Stat3 promotes the reduction of P-gp levels after restraining NF-κB. To further study the regulatory effect of NF-κB and Stat3 on P-gp expression, we used P65 siRNA (siP65) or Stat3 siRNA (siStat3) to knockdown P65 or Stat3 levels, respectively. Western blot analysis showed that after knockdown of P65 or Stat3, p-P65 or p-Stat3 levels were reduced separately (Fig. 4c). Knockdown of P65 blocked P-gp levels. Stat3 knockdown further enhanced the prohibitive effect of siP65 on P-gp expression (Fig. 4c, lanes 1, 2, 3, and 5). Furthermore, siP65 combined with siStat3 had stronger prevention of P-gp than Sch A (Fig. 4c, lanes 4 and 5).

We deduce that knockdown of Stat3 could promote the reversal effect of siP65 on MCF-7/DOX cells. MTT assay indicated that siP65 or siStat3 had the ability to reverse resistant MCF-7/DOX cells. Combined siP65 and siStat3 showed more potent anti-resistant effect on MCF-7/DOX cells than Sch A (Fig. 4c). These results demonstrate that Sch A inhibits p-P65 and p-Stat3, and decreased p-Stat3 enhances siP65-induced reversal effect on resistant MCF-7/DOX cells.

Discussion

We found that Sch A had reversal effect on several DOX-resistant cell lines, especially on MCF-7/DOX cell line (Fig. 1c). P-gp dramatically overexpressed in MCF-7/DOX cells, but not MRP1, MRP3 or even BCRP. Apparently, the resistance of MCF-7/DOX is due, at least in part, to high activity of P-gp pump. P-gp has been most extensively examined. Overexpression of P-gp has been shown to correlate with overall poor chemotherapy response and prognosis [16]. Thus, Sch A may be as a special inhibitor of P-gp to recover the sensitivity of MCF-7/DOX cells to DOX. Numerous strategies to overcome P-gp-dependent MDR have been explored, including the design of novel drugs that evade recognition and efflux, inhibitors to block efflux and restore drug accumulation [3]. P-gp inhibitors have been used with limited clinical success, as the co-administration of a cytotoxic drug with an inhibitor often produces undesirable or unpredictable pharmacokinetics [23]. In our manuscript, Sch

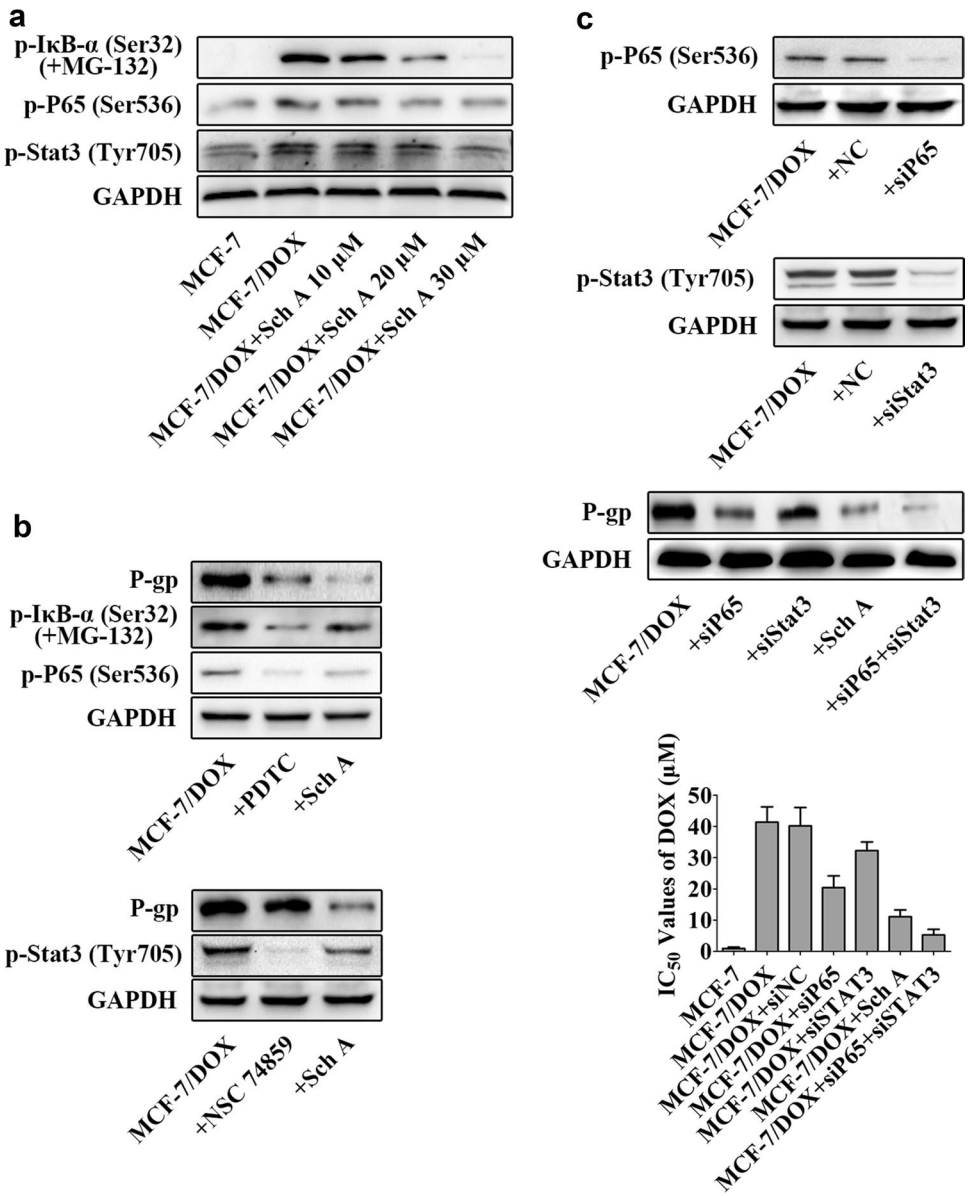

Fig. 4 Co-transfection with siStat3 and siP65 shows potent reverse effect on MCF-7/DOX cells. **a** Western blot results of the MCF-7 or MCF-7/DOX cells treated with 0–30 μM Sch A for 12 h. Where indicated, cells were also treated with the proteasome inhibitor MG-132 (10 μM). **b** Western blot results of the MCF-7/DOX cells treated with 20 μM PDTC for 1.5 h, 100 μM NSC 74859 for 12 h or 20 μM Sch A for 12 h. Where indicated, cells were also treated with the proteasome inhibitor MG-132 (10 μM). **c** MCF-7/DOX cells were transfected transiently with P65 siRNA (siP65), Stat3 siRNA (siStat3) or control siRNA (siNC), or co-transfected with siP65 and siStat3 for 48 h followed by Western blot analysis or MTT assay

A was tested for its reversal effect, cytotoxicity and inhibitory effect on P-gp. We found that Sch A was nontoxic to MCF-7 and MCF-7/DOX cells at the concentration below 50 μM (cell viability > 90%) (Fig. 1b), but showed significantly reversal effect on the resistance of MCF-7/DOX cells (Fig. 1d). Inhibitory effect of Sch A on P-gp is the main reason for reversal. DOX, a topoisomerase II inhibitor that is widely used in clinical treatments, is a substrate of P-gp in drug-resistant MCF-7 cells. It accumulates in nucleus to inhibit reconnection of DNA [24]. Due to the high level of P-gp, DOX was expelled and insufficient concentration was retained in MCF-7/DOX cells (Fig. 2a). Sch A suppressed P-gp (Figs. 2b, 3) and increased intracellular DOX accumulation (Fig. 2a), followed by enhancing DOX-induced apoptosis (Fig. 1e).

We demonstrated that NF-κB signaling and Stat3 signaling were activated in MCF-7/DOX cells compared with MCF-7 cells (Fig. 4a). To verify the relationship between NF-κB and P-gp, or between Stat3 and P-gp, specific NF-κB signaling inhibitor PDTC or specific Stat3 signaling inhibitor NSC 74859 were used, respectively. In PDTC treatment assay, the inhibition of P-gp levels was observed in MCF-7/DOX cells. Besides, with NSC 74859 incubation, P-gp levels were slightly reduced in MCF-7/DOX. Sch A showed more potent inhibition of P-gp than PDTC or NSC 74859, indicating the important role of NF-κB and Stat3 signaling in P-gp levels in MCF-7/DOX cells. SiRNA transfection confirmed this conclusion. NF-κB activation was inhibited by Sch A through canonical pathways (based on impeditive IκB-α-degradation that prevents NF-κB dimers, mainly

P65/P50 dimers, from accumulating in the nucleus and activate transcription) [25]. In the presence of the proteasome inhibitor MG-132, phosphorylation of IκB-α was detected in MCF-7/DOX cells (Fig. 4a, b). Stat3 activation requires phosphorylation of Tyr705, resulting in trans-modulation of downstream target genes that are involved in cell proliferation, survival, angiogenesis, and metastasis [26]. In the present study, Sch A inhibited Stat3 Tyr705 phosphorylation. Besides, siStat3 transfection reduced P-gp levels and promoted siP65-mediated P-gp down-regulation.

In conclusion, our findings demonstrate for the first time that Sch A specifically reverses P-gp-mediated DOX resistance in MCF-7/DOX cells by blocking P-gp, NF-κB, and Stat3 signaling. Furthermore, P-gp overexpressed in MCF-7/DOX cells but not MRP1, MRP3, or BCRP. In addition, siP65 needs siStat3 to enhance its inhibitory effect on P-gp levels. Bearing this effectiveness, the appropriate dose of Sch A has low toxicity in single treatment but could potently increase the sensitivity of MDR breast cancer to the chemotherapeutical drugs in clinical.

Compliance with ethical standards

Conflict of interest The authors declare that they have no competing interests.

References

1. Huang SD, Holzel M, Knijnenburg T, Schlicker A, Roepman P, McDermott U, et al. MED12 controls the response to multiple cancer drugs through regulation of TGF-beta receptor signaling. Cell. 2012;151:937–50.
2. Lee C, Park S, Kim JH, Lim SM, Park HS, Kim SI, et al. Expression of T-lymphocyte markers in human epidermal growth factor receptor 2-positive breast cancer. J Breast Cancer. 2016;19:385–93.
3. Xia YZ, Ni K, Guo C, Zhang C, Geng YD, Wang ZD, et al. Alopecurone B reverses doxorubicin-resistant human osteosarcoma cell line by inhibiting P-glycoprotein and NF-kappa B signaling. Phytomedicine. 2015;22:344–51.
4. Zhao XQ, Xie JD, Chen XG, Sim HM, Zhang X, Liang YJ, et al. Neratinib reverses ATP-binding cassette B1-mediated chemotherapeutic drug resistance in vitro, in vivo, and ex vivo. Mol Pharmacol. 2012;82:47–58.
5. Gillet JP, Gottesman MM. Overcoming multidrug resistance in cancer: 35 years after the discovery of ABCB1. Drug Resist Updat. 2012;15:2–4.
6. Kim SJ, Min HY, Lee EJ, Kim YS, Bae K, Kang SS, et al. Growth inhibition and cell cycle arrest in the G0/G1 by schizandrin, a dibenzocyclooctadiene lignan isolated from Schisandra chinensis, on T47D human breast cancer cells. Phytother Res. 2010;24:193–7.
7. Xia YZ, Yang L, Wang ZD, Guo C, Zhang C, Geng YD, et al. Schisandrin A enhances the cytotoxicity of doxorubicin by the inhibition of nuclear factor-kappa B signaling in a doxorubicin-resistant human osteosarcoma cell line. RSC Adv. 2015;5:13972–84.
8. Wang LJ, Meng Q, Wang CY, Liu Q, Peng JY, Huo XK, et al. Dioscin restores the activity of the anticancer agent adriamycin in multidrug-resistant human leukemia K562/adriamycin cells by down-regulating MDR1 via a mechanism involving NF-kappa B signaling inhibition. J Nat Prod. 2013;76:909–14.
9. Lu Y, Li F, Xu T, Sun J. Tetrandrine prevents multidrug resistance in the osteosarcoma cell line, U-2OS, by preventing Pgp overexpression through the inhibition of NF-kappaB signaling. Int J Mol Med. 2017;39:993–1000.
10. Assef Y, Rubio F, Colo G, del Monaco S, Costas MA, Kotsias BA. Imatinib resistance in multidrug-resistant K562 human leukemic cells. Leuk Res. 2009;33:710–6.
11. Watanabe A, Yamamoto K, Ioroi T, Hirata S, Harada K, Miyake H, et al. Association of single nucleotide polymorphisms in STAT3, ABCB1, and ABCG2 with stomatitis in patients with metastatic renal cell carcinoma treated with sunitinib: a retrospective analysis in Japanese patients. Biol Pharm Bull. 2017;40:458–64.
12. Zhang F, Wang Z, Fan Y, Xu Q, Ji W, Tian R, et al. Elevated STAT3 signaling-mediated upregulation of MMP-2/9 confers enhanced invasion ability in multidrug-resistant breast cancer cells. Int J Mol Sci. 2015;16:24772–90.
13. Johnston PA, Grandis JR. STAT3 signaling: anticancer strategies and challenges. Mol Interv. 2011;11:18–26.
14. Chiu LY, Ko JL, Lee YJ, Yang TY, Tee YT, Sheu GT. L-type calcium channel blockers reverse docetaxel and vincristine-induced multidrug resistance independent of ABCB1 expression in human lung cancer cell lines. Toxicol Lett. 2010;192:408–18.
15. Shi Z, Liang YJ, Chen ZS, Wang XW, Wang XH, Ding Y, et al. Reversal of MDR1/P-glycoprotein-mediated multidrug resistance by vector-based RNA interference in vitro and in vivo. Cancer Biol Ther. 2006;5:39–47.
16. Xia YZ, Yang L, Xue GM, Zhang C, Guo C, Yang YW, et al. Combining GRP78 suppression and MK2206-induced Akt inhibition decreases doxorubicin-induced P-glycoprotein expression and mitigates chemoresistance in human osteosarcoma. Oncotarget. 2016;7:56371–82.
17. Zhu FF, Dai CY, Fu YF, Loo JFC, Xia DJ, Gao SP, et al. Physalin A exerts anti-tumor activity in non-small cell lung cancer cell lines by suppressing JAK/STAT3 signaling. Oncotarget. 2016;7:9463–77.
18. Berger W, Setinek U, Hollaus P, Zidek T, Steiner E, Elbling L, et al. Multidrug resistance markers P-glycoprotein, multidrug resistance protein 1, and lung resistance protein in non-small cell lung cancer: prognostic implications. J Cancer Res Clin Oncol. 2005;131:355–63.
19. Bruhn O, Cascorbi I. Polymorphisms of the drug transporters ABCB1, ABCG2, ABCC2 and ABCC3 and their impact on drug bioavailability and clinical relevance. Expert Opin Drug Metab Toxicol. 2014;10:1337–54.
20. Robey RW, Ierano C, Zhan Z, Bates SE. The challenge of exploiting ABCG2 in the clinic. Curr Pharm Biotechnol. 2011;12:595–608.
21. Guo Y, Ding Y, Zhang T, An H. Sinapine reverses multidrug resistance in MCF-7/dox cancer cells by downregulating FGFR4/FRS2alpha-ERK1/2 pathway-mediated NF-kappaB activation. Phytomedicine. 2016;23:267–73.
22. Liu J, Zhou F, Chen Q, Kang A, Lu M, Liu W, et al. Chronic inflammation up-regulates P-gp in peripheral mononuclear blood cells via the STAT3/Nf-kappab pathway in 2,4,6-trinitrobenzene sulfonic acid-induced colitis mice. Sci Rep. 2015;5:13558.
23. Krishna R, Mayer LD. Multidrug resistance (MDR) in cancer. Mechanisms, reversal using modulators of MDR and the role of MDR modulators in influencing the pharmacokinetics of anticancer drugs. Eur J Pharm Sci. 2000;11:265–83.

24. Gill J, Ahluwalia MK, Geller D, Gorlick R. New targets and approaches in osteosarcoma. Pharmacol Ther. 2013;137:89–99.
25. Campbell KJRS, Perkins ND. Active repression of antiapoptotic gene expression by RelA(p65) NF-kappa B. Mol Cell. 2004;13:853–65.
26. Narayanan PD, Nandabalan SK, Baddireddi LS. Role of STAT3 phosphorylation in ethanol-mediated proliferation of breast cancer cells. J Breast Cancer. 2016;19:122–32.